A new reactive absorption model using extents of reaction and activities. II. Application to CO 2 absorption into aqueous MDEA solutions

Serena Delgado, Alain Gaunand, Christophe Coquelet, Renaud Cadours, Céline Volpi

A new reactive absorption model using extents of reaction and activities. II. Application to CO_2 absorption into aqueous MDEA solutions

Serena Delgado[a], Alain Gaunand[a]*, Christophe Coquelet[a,c]*, Renaud Cadours[a,b] and Céline Volpi[b]

[a] *Mines Paris, PSL University, CTP (Centre of Thermodynamics of Processes) 35 Rue Saint Honoré 77305 Fontainebleau Cedex, France*

[b] *TotalEnergies SE, Tour Coupole, 2 place Jean Millier, 92078 Paris La Défense Cedex, France*

[c] *Université de Toulouse, IMT Mines Albi, CNRS UMR 5302, Centre Rapsodee Campus Jarlard, 81013 Albi CT Cedex 9, France*

**Corresponding authors e-mail addresses: alain.gaunand@minesparis.psl.eu, christophe.coquelet@mines-albi.fr.*

Keywords

Gas-liquid absorption, Kinetic model, Non ideality, MDEA solution, CO_2 absorption

Abstract

Absorption into basic aqueous solutions is widely used for CO_2 separation from raw natural gas or from flue gases. This study implements a general steady-state model for reactive gas-liquid absorption. This work expands upon a first case study where the model was applied with the stagnant film theory (Whitman, 1923) to alkaline salts-water-CO_2 systems. This second case study uses the resulting Arrhenius expression to examine published CO_2 absorption and desorption flux data in MDEA-water-CO_2 system. Arrhenius parameters are optimised for the reaction CO_2 + MDEA + $H_2O \leftrightarrow HCO_3^-$ + $MDEAH^+$ with lnk ($m^3.mol^{-1}.s^{-1}$) = 16.69 – 6385/T (K). Results emphasise the role of CO_2 physical solubility representation in reactive absorption model overall performance. Global modelling is needed: kinetic parameters should be used together with all underlying parameters with which they were obtained. The relevance of activity-based modelling is shown, especially at high CO_2 absorption/desorption driving force.

Nomenclature

A	Logarithm of Arrhenius pre-exponential factor
c_i	Molar concentration of species i ($mol.m^{-3}$)
$c_{1,0}$	Concentration of absorbed gas at gas-liquid interface ($mol.m^{-3}$)
$c_{abs,tot}$	Total absorptive species concentration ($mol.m^{-3}$)
C_i	Normalised concentration of species i (-)
E_A	Activation energy ($J.mol^{-1}$)
E'	Flux density (-)
f_{obj}	Optimisation objective function (-)
H_1	Henry's constant of absorbed gas at infinite dilution (Pa)
j_i	Flux of species i through liquid film ($mol.m^{-2}.s^{-1}$)
k_j	Reaction j kinetic constant
K_j	Reaction j equilibrium constant
$k_{L,1}$	Liquid-side mass transfer coefficient regarding the absorbed gas ($m.s^{-1}$)
n_C	Number of solute constituents in liquid phase
$n_{R,kin}$	Number of finite-rate reactions in the reaction mechanism
$n_{R,eq}$	Number of reactions at equilibrium in the reaction mechanism
P	Pressure (Pa)
Re	Reynolds number
r_j	Reaction rate of reaction j ($mol.m^{-3}.s^{-1}$)
Sc	Schmidt number
Sh	Sherwood number
T	Temperature (K)

Constants

R	Ideal gas constant ($J.mol^{-1}.K^{-1}$)

Greek letters

α	CO_2 loading in solution ($mol.mol\ MDEA^{-1}$)
γ_i	Activity coefficient of species i (-)
μ_S	Solution viscosity (Pa.s)
ξ_j	Extent of reaction j (-)
ρ_S	Solution density ($kg.m^{-3}$)
ω_i	Mass fraction of species i (-)
$\omega_{MDEA,app}$	Apparent mass fraction of MDEA (equivalent MDEA mass fraction of a given solution at zero CO_2 loading)

Subscripts and superscripts

app	Apparent (=in equivalent unloaded solution)
calc	Calculated
eq	At equilibrium
exp	Experimental
0	At interface
1	Absorbed gas
~c	Molar concentration-based symmetric thermodynamic convention

1. Introduction

Chemical absorption of CO_2 into basic solutions has been in use since the 1930s for its separation from raw natural gas of from flue gases (Bottoms 1931). Solvent screening and design are at the heart of the research effort to increase both CO_2 absorption rate and capacity, and to decrease solvent regeneration duty (e.g., aqueous amine blends). Kinetic parameters are typically obtained from absorption or desorption flux measurements in laboratory gas-liquid contactors of known mass transfer coefficient and interfacial area.

Experiments should be carried out as close to industrial conditions as possible (amine content, CO_2 partial pressure and loading, temperature). Yet, most kinetic studies deal with absorption experiments into unloaded basic solutions. Only one irreversible reaction is considered between absorbed gas and amine (e.g., (Pohorecki et Moniuk 1988), (Pani, et al. 1997), (Derks, et al. 2006)). Moreover, rate expressions are based on molarities. However, when CO_2 is absorbed, bicarbonate, carbonate and carbamate ions are formed. This increases ionic strength, and solution non ideality as well. Therefore, absorption models based on activities rather than molarities should lead to more relevant process simulation.

CO_2 reaction with hydroxide ion HO^- takes place in all aqueous systems with CO_2. In amine-based solutions, its rate cannot always be disregarded compared to that of CO_2 reaction with the amine species. Furthermore, through molecular simulation, (Rozanska, Wimmer et de Meyer 2021) show that CO_2 kinetics in aqueous tertiary amine solutions can be written as a function of CO_2 and HO^- concentrations only. For pilot effective mass transfer area measurement by CO_2 absorption into NaOH solutions, (Sheng, et al. 2019) obtain large deviations in estimated area based on five literature kinetic constants. They additionally conclude that inconsistencies between kinetic and physical parameter sources should be avoided. The need for global modelling is emphasised.

For these reasons, part I of the present work focused on CO_2 absorption kinetics into alkaline salts solutions (Delgado, et al. 2023). It introduced a reactive absorption model where equilibrium relations, Nernst-Planck diffusion fluxes and reaction rates are written based on activities. This model can be applied in any chemical system and to validate any reaction mechanism. For steady-state mass transfer representations, local fluxes are related by stochiometric constraints through extents of reactions and ensure mass conservation. This significantly reduces the number of differential equations to solve. This model with the stagnant film theory (Whitman, 1923) was then applied to alkaline salts-water-CO_2 systems for validation. Arrhenius parameters of the direct kinetic constant of reaction $CO_2 + HO^- \leftrightarrow HCO_3^-$ were obtained in the 298-338 K temperature range. Resulting values were coherent with previous works.

Following this first case study, the purpose of this article is to apply the developed general reactive absorption model to CO_2 absorption and desorption in aqueous N-methyldiethanolamine (MDEA) solutions. Both CO_2 reactions with MDEA and with hydroxide ion are considered, so that their individual contribution to absorption can be quantified. Most available literature datasets are included, covering broad experimental condition ranges (see Table 1). The last column indicates the number of available CO_2 absorption and/or desorption flux measurements.

Table 1 Summary of lab-scale CO_2 absorption studies in aqueous MDEA solutions

Ref, apparatus	$\omega_{MDEA,app}$	α (mol.mol $MDEA^{-1}$)	T (K)	P_{CO2} (kPa)	n_{data}
(Rinker, Sami et Sandall 1995), SC	0.1-0.3	0	293-342	72-100	21
(Pani, et al. 1997), LC	0.1-0.52	0	295-344	100-196	34
(Cadours 1998), LC	0.25-0.5	0.02-0.85	312-383	2.3-1757	114
(Ko et Li 2000), WWC	0.12-0.29	0.01-0.03	303-313	37-98	12
(Pacheco et Kaganoi 2000), WWC	0.35-0.5	0.03-0.32	298-373	67-748	9
(Benamor et Aroua 2007), LC	0.12-0.46	0-0.17	293-323	9.1-59	99
(Camacho, et al. 2009), LC	0.009-0.38	0	288-313	88-95	42
(Qian et Guo 2009), WWC	0.1-0.3	0.01-0.04	300-313	94-98	12
(Kierzkowska-Pawlak et Chacuk 2010), LC	0.1-0.2	0	293-333	26-108	30
(Hamborg et Versteeg 2012), LC	0.23	0-0.8	298-333	1.7-136	21
(Costa, et al. 2019), MC	0.12-0.35	0	298	14	3

HSC: "Hemispherical Contactor", LC: "Lewis Cell", MC: "Membrane Contactor", SC: "Spherical Wetted-Wall Contactor", WWC: "Wetted-Wall Column"

Firstly, a data coherence analysis over available absorption and desorption flux measurements is carried out (section 2). It consists in a graphical analysis of flux density E' (see eq. 1) as a function of temperature and CO_2 loading. Outlier points are identified and filtered out. Over the consolidated dataset, the model is then applied to CO_2 absorption and desorption in aqueous MDEA solutions with a complete reaction mechanism considering four reversible reactions (two finite rate reactions and two acid-base equilibria). This third section aims at fitting the parameters of an Arrhenius-type expression for the direct kinetic constant of reaction CO_2 + MDEA + H_2O ↔ $MDEAH^+$ + HCO_3^-. Optimisation is carried out in both concentration- and activity-based modelling frameworks. Kinetic parameters of CO_2 reaction with hydroxide ion from (Delgado, et al. 2023) are reused here. An overall average absolute deviation (AAD) of calculated to experimental fluxes of 12% was obtained in (Delgado, et al. 2023), with slightly better performance than (Gondal, Svendsen et Knuutila 2016).

2. Data coherence analysis

Flux density E' of an absorption or desorption experiment is defined in eq. (1).

$$E' = \frac{j_{\mathrm{CO_2,exp}}}{\frac{k_{\mathrm{L,CO_2}}}{H_{\mathrm{CO_2,app}}}\left(p_{\mathrm{CO_2,0}} - p_{\mathrm{CO_2,eq}}\right)} \quad (1)$$

Where, for a given data point, flux density E' is a normalised flux considering proximity to equilibrium. $j_{CO2,exp}$, the algebraic experimental CO_2 absorption (>0) or desorption (<0) flux, $k_{L,CO2}$, the liquid-side CO_2 mass transfer coefficient, and $p_{CO2,0}$, the CO_2 partial pressure at gas-liquid interface are provided by literature sources. $H_{CO2,app,}$ the apparent Henry's constant of CO_2, is calculated with the correlation by (Vinel et Bouallou 2004), and $p_{CO2,eq}$, the equilibrium CO_2 partial pressure, is

calculated as a function of experimental conditions with the thermodynamic model described in the Supplementary Material.

This variable can be read as a comparison of chemical absorption or desorption flux $j_{\mathrm{CO_2,exp}}$ to a physical absorption flux in an equivalent non-reactive system $\frac{k_{\mathrm{L,CO_2}}}{H_{\mathrm{CO_2,app}}}\left(p_{\mathrm{CO_2,0}} - p_{\mathrm{CO_2,eq}}\right)$. Moreover, flux density is always positive. Therefore, CO_2 absorption and desorption data can be represented and compared on one diagram.

E' is plotted as a function of CO_2 loading and at different MDEA concentration levels in Figure 1. Datasets are sorted according to five rounded apparent MDEA mass fraction. Colours reflect four different temperature intervals.

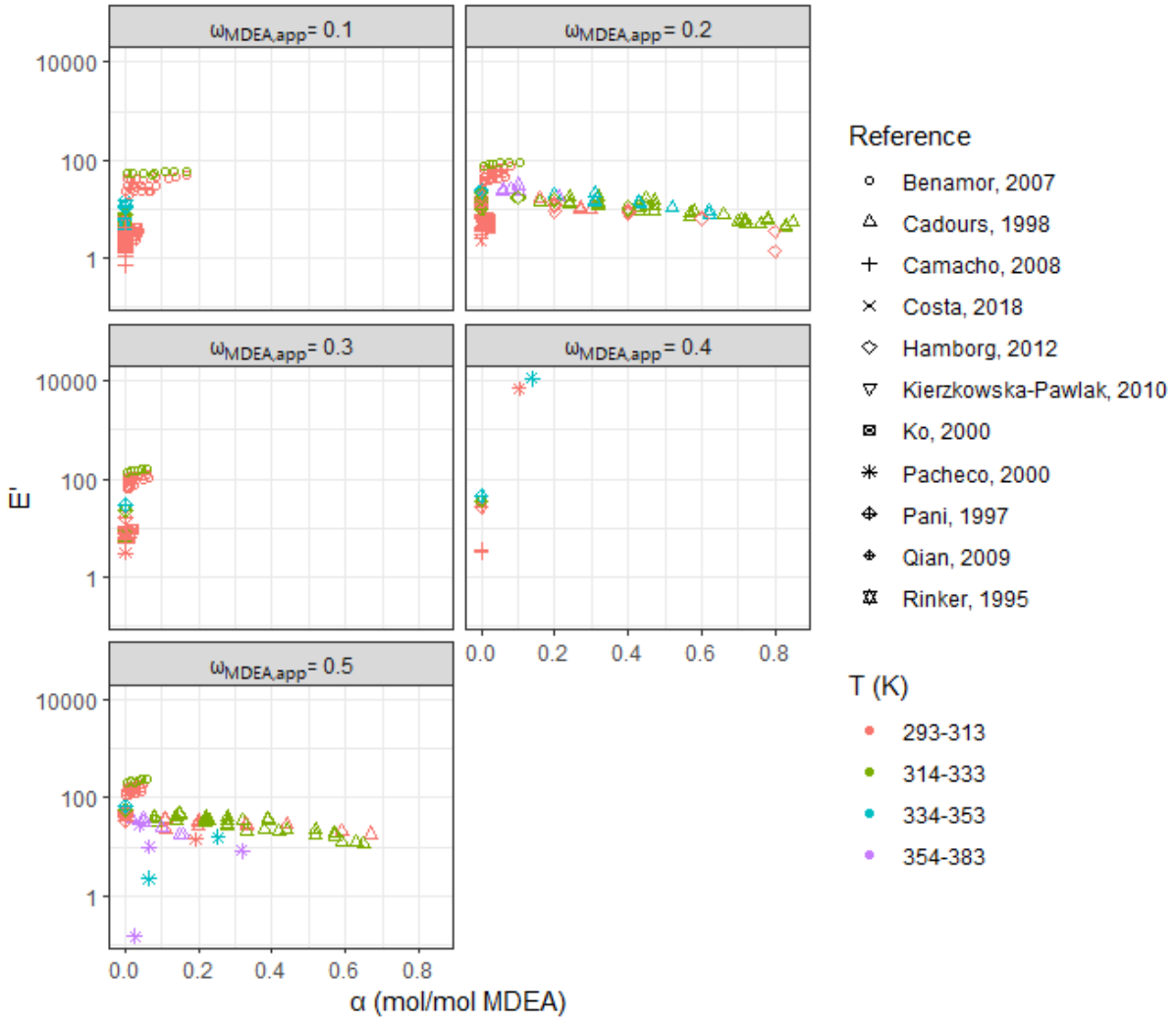

Figure 1 Graphical coherence analysis of available CO_2 absorption and desorption flux data in aqueous MDEA solutions as a function of CO_2 loading and apparent MDEA mass fraction $\omega_{\mathrm{MDEA,app}}$

Figure 1 shows a decreasing trend of flux density with increasing CO_2 loading at 0.2 and 0.5 MDEA mass fractions. Data are mostly available in unloaded solutions, where flux density spans a wide

interval. This can stem from variability between data sources and visualising all temperatures in the same plot. The choice of thermodynamic representation could also play a role in this result.

Outlier points are mainly from two references. On the one hand, flux density of (Benamor et Aroua 2007) data is systematically above that of other data sources in unloaded solutions and remains constant or increases slightly with increasing CO_2 loading. This behaviour is incompatible with other data sources. Therefore, absorption flux measurements by (Benamor et Aroua 2007) are not selected in the following section.

On the other hand, outlier points from (Pacheco et Kaganoi 2000) data at 0.4 MDEA mass fraction have flux densities close to 1.10^4 whereas flux densities from other sources are not over 1.10^2. At 0.5 MDEA mass fraction, another of their points stands out with a flux density around 0.1 at low CO_2 loading whereas it is not below 1 in other sources. Three more points stand out from the trend outlined by the data from (Cadours 1998) and (Hamborg et Versteeg 2012) with a higher flux density of around 10 that remains constant regardless of temperature or CO_2 loading. Considering outliers represent more than half of the data from (Pacheco et Kaganoi 2000), their absorption flux measurements are not selected either in section 3.

Figure 2 focuses on calculated flux density from (Cadours 1998) and (Hamborg et Versteeg 2012) data as a function of CO_2 loading at $\omega_{MDEA,app}$ = 0.23-0.25. Activity-based model trend is also represented with the kinetic parameters determined in section 3. Flux density tends to decrease with growing CO_2 loading, as in Figure 1. However, data from (Hamborg et Versteeg 2012) systematically display lower densities than the trend of (Cadours 1998). Selected data sources for CO_2-loaded solutions appear incompatible. Both were kept in section 3 because of missing discrimination method, such as a third data source with CO_2-loaded solutions.

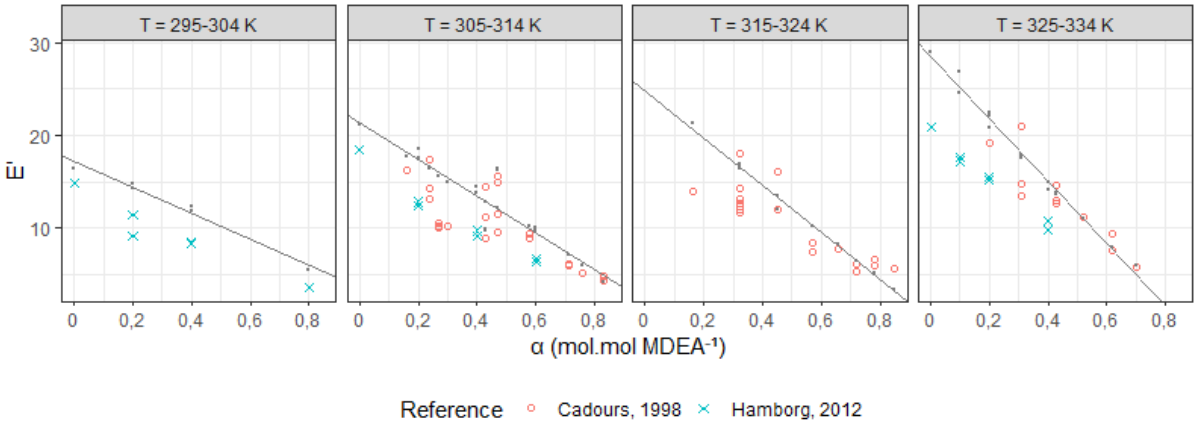

Figure 2 (Cadours 1998) and (Hamborg et Versteeg 2012) data flux density as a function of CO_2 loading at $\omega_{MDEA,app}$ = 0.23-0.25. Grey dots and lines: activity-based model flux density and trend.

3. Application to MDEA-water-CO_2 system

The mass transfer modelling framework is described in part I of the present work (Delgado, et al. 2023). Therefore, only MDEA-specific parameters are specified in the following section (see Supplementary Material section 1 and (Delgado, et al. 2023) for modelling framework description).

In this system, six species are considered: CO_2, HCO_3^-, CO_3^{2-}, MDEA, $MDEAH^+$ and HO^- (n_C=6). The mechanism consists in four reversible reactions (n_R=4):

$$CO_2 + MDEA + H_2O \leftrightarrow MDEAH^+ + HCO_3^- \quad \text{(R-I)}$$
$$CO_2 + HO^- \leftrightarrow HCO_3^- \quad \text{(R-II)}$$
$$HCO_3^- + HO^- = CO_3^{2-} + H_2O \quad \text{(R-III)}$$
$$MDEAH^+ + HO^- = MDEA + H_2O \quad \text{(R-IV)}$$

Reactions R-I and R-II are reversible and with finite rate ($n_{R,kin}$=2). As in most studies, a direct CO_2 reaction with MDEA is considered according to the mechanism proposed by (Donaldson et Nguyen 1980).

$$r_I = r_{(CO_2,MDEA)} = \tilde{k}^c_{(CO_2,MDEA)} \left(\tilde{\gamma}_{CO_2} \tilde{\gamma}_{MDEA} c_{CO_2} c_{MDEA} - \frac{\tilde{\gamma}_{(MDEAH^+)} c_{(MDEAH^+)} \tilde{\gamma}_{(HCO_3^-)} c_{(HCO_3^-)}}{\tilde{K}^c_{(CO_2,MDEA)}} \right) \quad (2)$$

$$r_{II} = r_{(CO_2,HO^-)} = \tilde{k}^c_{(CO_2,HO^-)} \left(\tilde{\gamma}_{CO_2} \tilde{\gamma}_{(HO^-)} c_{CO_2} c_{(HO^-)} - \frac{\tilde{\gamma}_{(HCO_3^-)} c_{(HCO_3^-)}}{\tilde{K}^c_{(CO_2,HO^-)}} \right) \quad (3)$$

Where $\tilde{k}^c_{(CO_2,MDEA)}$ and $\tilde{k}^c_{(CO_2,HO^-)}$ ($m^3.mol^{-1}.s^{-1}$) are the forward kinetic constants of reactions R-I and R-II, and $\tilde{K}^c_{(CO_2,MDEA)}$ (dimensionless) and $\tilde{K}^c_{(CO_2,HO^-)}$ ($m^3.mol^{-1}$) are their equilibrium constants. $\tilde{k}^c_{(CO_2,MDEA)}$ is the constant to determine. ~c refers to the molar concentration-based symmetric thermodynamic convention (see eq. SM24 and following in Supplementary Material).

In addition, acid-base equilibria between HCO_3^- and CO_3^{2-} (reaction R-III) and $MDEAH^+$ and MDEA (reaction R-IV) are considered ($n_{R,eq}$=2). Equilibrium constant parameters of reactions R-II and R-III are taken from (Kamps, Balaban, et al. 2001). (Kamps et Maurer, 1996) provides equilibrium constant parameters of reactions R-I and R-IV.

New correlations have been developed for density and viscosity of both CO_2-unloaded and -loaded solutions. CO_2 and MDEA liquid phase diffusion coefficients are calculated using modified Stokes-Einstein relations (Versteeg et Van Swaaij, Solubility and diffusivity of acid gases (carbon dioxide, nitrous oxide) in aqueous alkanolamine solutions 1988). All ionic species are assumed to have the same diffusivity as MDEA (see Supplementary Material section 1 for detailed correlations). As stated in part I of the present work, the necessary data to implement a distinction in ionic diffusivities is not available. Ionic diffusivities are primarily measured at infinite dilution. However, they are expected to depend on the composition of the solution, but these effects have not been measured in ionic systems. The current assumption is a result of the lack of data. Moreover, this effect is expected to be small compared to the uncertainty of CO_2 absorption and desorption flux measurements and of relevant physico-chemical parameters like viscosity.

As a base case, the mass transfer model is tested with no deviation from ideality. This modelling framework is denoted "concentration-based model". N_2O physical solubility in aqueous MDEA solutions is calculated with the correlation of (Vinel et Bouallou 2004). CO_2 Henry's constant is calculated with the so-called CO_2-N_2O analogy. Since the physical solubility correlation only considers unloaded solutions, this base case is applied to low-loading flux data ($\alpha \leq 0.05$ mol.mol MDEA^{-1}).

Secondly, the activity-based model is implemented. Equilibria and solution non-ideality are represented with one thermodynamic model, described in the Supplementary Material. Thus, all selected datapoints in CO_2-unloaded and -loaded solutions are considered. Several hundred CO_2 absorption and desorption flux measurements are available in the literature, from a variety of gas-liquid contactors over broad ranges of operating conditions (293-383 K, 0.009-0.52 apparent MDEA mass fraction, 0-0.85 mol.mol MDEA^{-1} CO_2 loading and 0.2-1757 kPa CO_2 partial pressure).

The pre-exponential factor A and the temperature of activation E_A/R of reaction R-I direct kinetic constant are fitted. The Arrhenius equation is shown in eq. (4) and the objective function is specified in eq. (5).

$$\ln k_{(\mathrm{CO_2,MDEA})} = A - \frac{E_A}{RT} \tag{4}$$

$$f_{\mathrm{obj}} = \sum_{i\ \mathrm{points}} \frac{1}{2}\left(\left(\frac{j_i^{\mathrm{calc}} - j_i^{\mathrm{exp}}}{j_i^{\mathrm{exp}} + s\varepsilon}\right)^2 + \left(\frac{j_i^{\mathrm{calc}} - j_i^{\mathrm{exp}}}{j_i^{\mathrm{calc}} + s\varepsilon}\right)^2\right) \tag{5}$$

Where j is the CO_2 absorption flux and ε is a constant set to 1.10^{-4} to mitigate error value for very small absorption fluxes. Because both absorption and desorption fluxes are available in this system, a factor s represents the experimental flux sign (s=1 if $j_i^{exp} > 0$, -1 otherwise). As indicated in (Delgado, et al. 2023), the two terms give this objective function a symmetric behaviour regarding flux underestimation and overestimation. Optimisation function fminsearch in Matlab R2013a is used to adjust Arrhenius parameters of the kinetic constant. This function implements the simplex algorithm by (Lagarias, et al. 1998).

Model application to selected flux measurements aims at optimising Arrhenius parameters of the direct kinetic constant of reaction R-I to minimise f_{obj}. Arrhenius parameters obtained in (Delgado, et al. 2023) are used for the direct kinetic constant of reaction R-II.

Table **2** and Figure 3 compare adjusted Arrhenius parameters in each modelling approach to previous studies. The concentration-based model leads to similar Arrhenius parameters to (Littel, Van Swaaij et Versteeg 1990), (Rangwala, et al. 1992), (Pani, et al. 1997), (Kierzkowska-Pawlak et Chacuk 2010) and (Jamal, Meisen et Lim 2006). On the other hand, the activity-based model leads to higher values for A and E_A/R compared to Arrhenius parameters of previous studies. For instance, the resulting kinetic constant is 1.8 times higher than that of (Jamal, Meisen et Lim 2006) over the entire temperature interval. The higher activity-based model kinetic constant can be caused by a product of CO_2 and MDEA activity coefficients lower than one. It can also stem from the different representation of equilibria, with lower calculated absorption/desorption driving force in the activity-based model compared to the concentration-based model. As will be seen in Figure 7 and Figure 8, driving force is indeed lower according to the activity-based model. Among the listed studies, the activity-based model in the present work is the only modelling framework considering system deviation from ideality through the liquid film. Only in (Cadours 1998) and (Hamborg et Versteeg 2012) is CO_2 loading factored in CO_2 Henry's constant, by an ionic-strength-dependent correction factor or an experimental assessment with the N_2O-CO_2 analogy (see Table 2).

239 **Table 2** Resulting Arrhenius parameters for the direct kinetic constant of reaction R-I and comparison to previous studies

Reference	A	E_A/R (K)	T (K)	Transfert model	Non-ideality representation	Reactions
Activity-based model	16.69	6385	293-383	Film	Deshmukh-Mather	I-IV
Concentration-based model	13.60	5567	293-383	Film	Ideal solution	I-IV
(Versteeg et van Swaaij 1988)	11.69	5103	293-333	Penetration	Ideal solution	I, II, V
(Tomcej et Otto 1989)	11.99	5134	298-348	Film (pfo)	Ideal solution	I, II, V
(Littel, Van Swaaij et Versteeg 1990)	14.11	5771	293-333	Penetration	Ideal solution	I, II
(Rangwala, et al. 1992)	13.96	5770	298-333	Film (pfo)	Ideal solution	I
(Rinker, Sami et Sandall 1995)	10.28	4579	293-343	Penetration	Ideal solution	I-IV, VI
(Pani, et al. 1997)	13.06	5461	296-343	Film	Ideal solution	I
(Cadours 1998)	12.60	5333	296-343	Film	H_{CO2} = f(I)	I
(Ko et Li 2000)	12.90	5400	303-313	Film	Ideal solution	I, II
(Jamal, Meisen et Lim 2006)	14.51	5798	303-353	Penetration	Ideal solution	I-IV, VI
(Camacho, et al. 2009)	15.49	6244	288-313	Film	Ideal solution	I,II
(Qian et Guo 2009)	12.28	5190	300-313	Penetration	Ideal solution	I-VI
(Kierzkowska-Pawlak et Chacuk 2010)	14.54	5913	293-333	Film	Ideal solution	I
(Hamborg et Versteeg 2012)	9.72	4504	298-333	Penetration	Ideal solution*	I-IV, VI

pfo: "pseudo-first order", H_{CO2}: CO_2 Henry's constant, I: ionic strength

* (Hamborg et Versteeg 2012) experimentally assess H_{N2O} in CO_2-loaded solution and use the N_2O-CO_2 analogy to calculate H_{CO2}

Reactions: (V) $CO_2 + H_2O \leftrightarrow HCO_3^- + H^+$, (VI) $2H_2O = HO^- + H_3O^+$

240

241

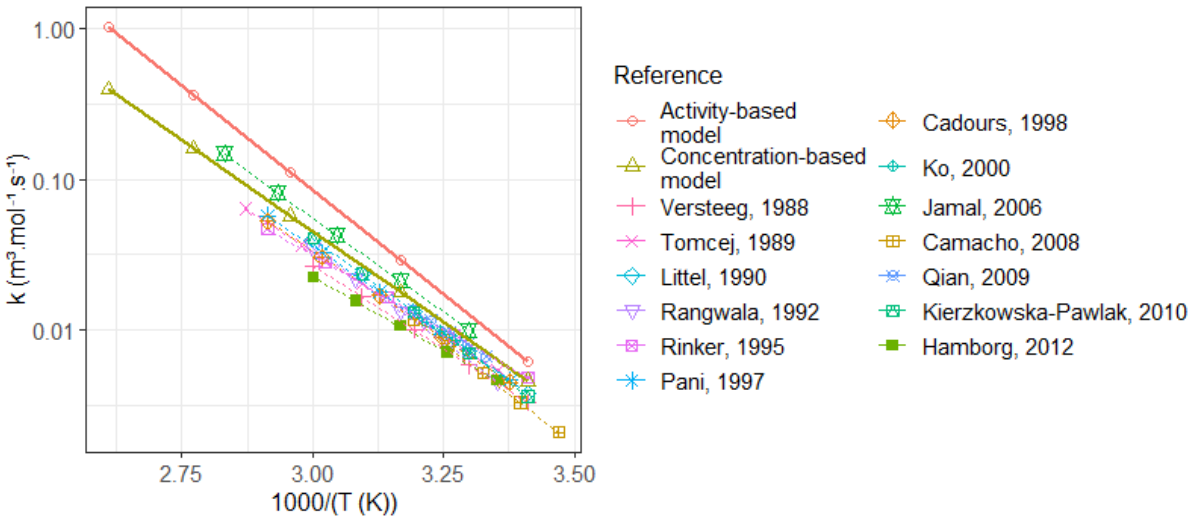

Figure 3 Arrhenius plots obtained in concentration-based and activity-based modelling frameworks and in previous studies for the direct kinetic constant of reaction R-I

Model performance criteria are presented in Table 3, including average absolute deviation (AAD, eq. (6)) and bias (eq. (7)).

$$\mathrm{AAD} = \frac{1}{n_{\mathrm{data}}} \sum_{i\ \mathrm{data}} \left| \frac{j_i^{\mathrm{calc}} - j_i^{\mathrm{exp}}}{j_i^{\mathrm{exp}}} \right| \times 100 \tag{6}$$

$$\mathrm{bias} = \frac{1}{n_{\mathrm{data}}} \sum_{i\ \mathrm{data}} \frac{j_i^{\mathrm{calc}} - j_i^{\mathrm{exp}}}{j_i^{\mathrm{exp}}} \times 100 \tag{7}$$

Table 3 Mass-transfer modelling performance for MDEA-water-CO_2 system

(%) Model		Concentration-based (α ≤ 0.05)		Activity-based (all selected data)	
Reference		AAD	Bias	AAD	Bias
(Rinker, Sami et Sandall 1995)		9	-9	11	-5
(Pani, et al. 1997)		11	-10	17	-17
(Cadours 1998)		29	29	17	0.8
(Ko et Li 2000)		15	-15	17	-17
(Camacho, et al. 2009)		17	16	20	20
(Qian et Guo 2009)		11	-11	13	-13
(Kierzkowska-Pawlak et Chacuk 2010)		6	2	10	9
(Hamborg et Versteeg 2012)		20	20	42	42
(Costa, et al. 2019)		24	-24	35	-35
Overall	α ≤ 0.05	12	-0.6	16	-0.2
	All selected data	-	-	18	3

Parity and deviation plots are shown in Figure 4, Figure **5** and Figure 6.

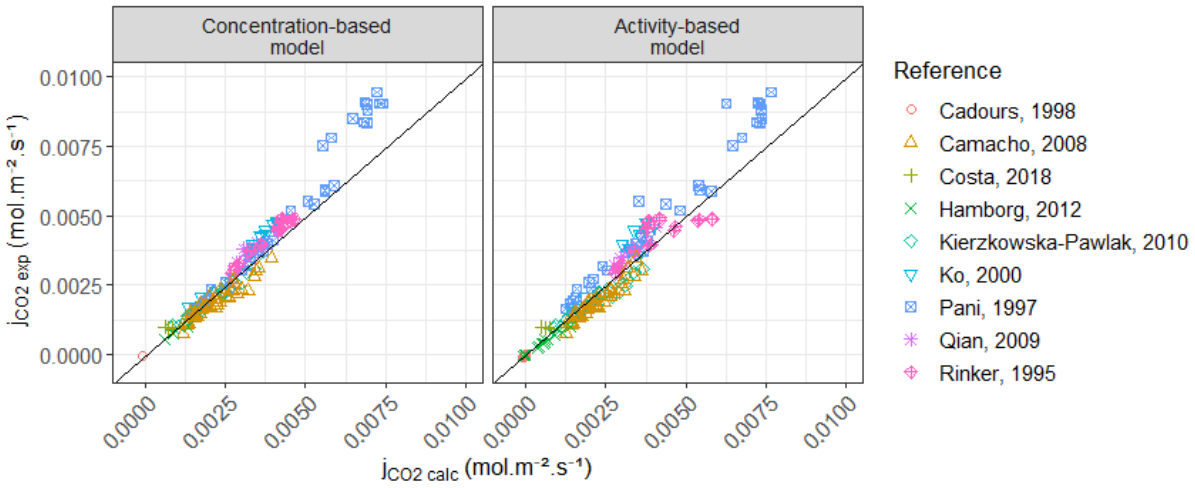

250

251 **Figure 4** Reactive absorption model parity plot for MDEA-water-CO_2 system. Concentration-based
252 model: $\alpha \leq 0.05$, activity-based model: all selected data.

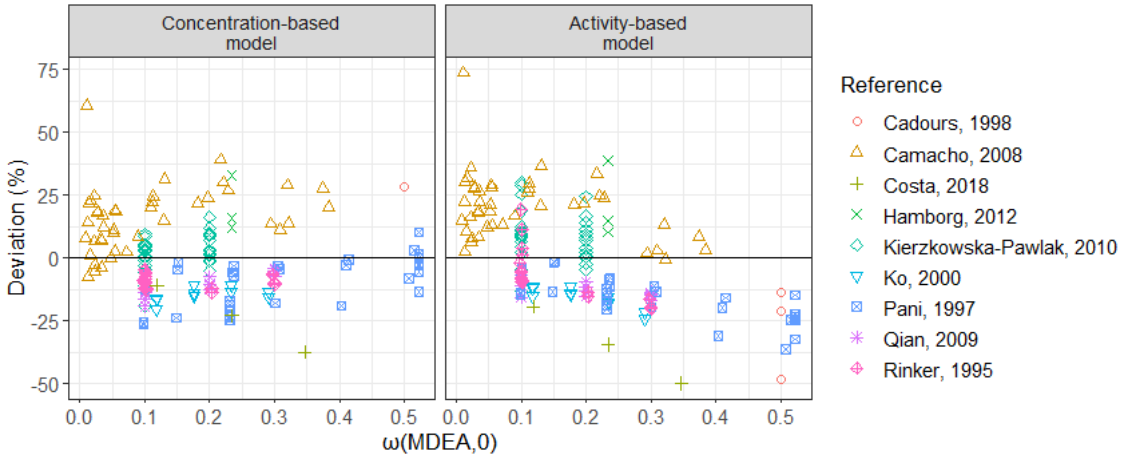

253

254 **Figure 5** Reactive absorption model deviations for MDEA solutions at low CO_2 loading ($\alpha \leq 0.05$)

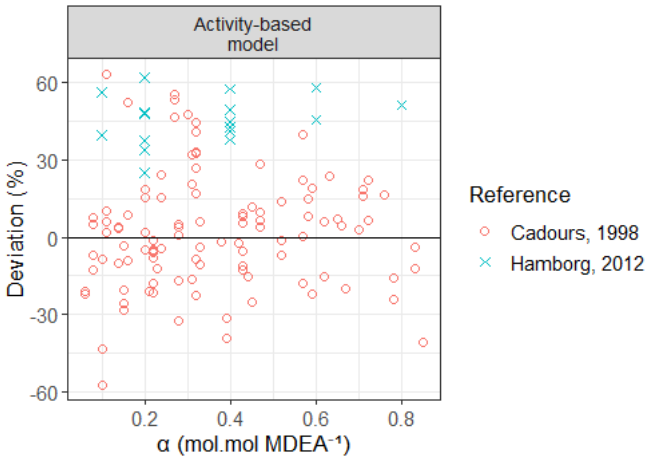

255

256 **Figure 6** Reactive activity-based absorption model deviations for MDEA solutions at high CO_2 loading
257 ($\alpha > 0.05$)

Both approaches give reliable representation of selected data at low CO_2 loading (AAD 12% vs. 16%). Figure 5 shows (Camacho, et al. 2009) data is better represented by activity-based model when amine mass fraction increases, whereas (Pani, et al. 1997) data is increasingly underestimated with this model. The concentration-based model results in slightly better performance at low CO_2 loading, but the activity-based model considers non-ideality with a unique thermodynamic model: (1) in diffusion via Nernst-Planck equation, (2) in kinetics via activity-based rates of reactions and (3) in equilibria as part of the selected thermodynamic representation. Moreover, the use of CO_2 solubility correlations based on N_2O-CO_2 analogy is avoided. This is a major advantage for model generality.

The main area for improvement of the activity-based model concerns the thermodynamic representation of the system, specifically that of CO_2 physical solubility in solution. Indeed, Henry's constant in solution is calculated based on CO_2 Henry's constant in pure water (see Supplementary Material). It might be beneficial to consider amine concentration as well instead of simply correcting Henry's constant in pure water by the CO_2 activity coefficient factor. (Zhang et Chen 2011) achieve this by introducing a mixing rule for CO_2 Henry's constant normalised by solute activity coefficient at infinite dilution in each component of the solvent.

At high CO_2 loading (see Figure 6), (Cadours 1998) data is well represented by the activity-based model. Absorption and desorption flux measurements by (Hamborg et Versteeg 2012) are systematically overestimated by the activity-based model (bias=AAD=42%). This is coherent with previous observations of the incompatibility of the two datasets in the data coherence analysis (see Figure 2). Optimisation currently favours (Cadours 1998) data representation because of the difference in data point numbers between the two sources (114 vs. 21).

Activity-based model results at specific conditions are then examined (Figure 7 to Figure 10, conditions listed in Table 4). The four selected points cover the examined data experimental conditions (MDEA concentration, temperature, CO_2 partial pressure and loading, absorption and desorption experiments). For each point, normalised concentration, extent of reaction and activity coefficient profiles obtained with the activity-based model are plotted. In unloaded solutions, concentration-based model normalised concentration and extent of reaction profiles are also plotted in dashed lines. As a reminder, CO_2 concentration is normalised by $c_{1,0}$, its interfacial concentration, while all other concentrations are normalised by $c_{abs,tot} = c_{MDEA,app}$.

Table 4 Conditions of selected points for concentration, extent of reaction and activity coefficient profile simulation

Figure	Reference	$\omega_{MDEA,app}$	α	T (K)	P_{CO2} (kPa)	$k_{L,1}$ ($m.s^{-1}$)	$c_{1,0}$ ($mol.m^{-3}$)*
Figure 7	(Qian et Guo 2009)	0.10	0.03	300	94.6	$5.38.10^{-5}$	24.3
Figure 8	(Pani, et al. 1997)	0.51	0	318	104.9	$5.43.10^{-6}$	6.3
Figure 9	(Cadours 1998)	0.50	0.28	332	70.1	$9.44.10^{-6}$	5.1
Figure 10	(Hamborg et Versteeg 2012)	0.23	0.10	333	22.6	$1.84.10^{-5}$	2.7

*Calculated variable (see (Delgado, et al. 2023)), in the activity-based model framework.

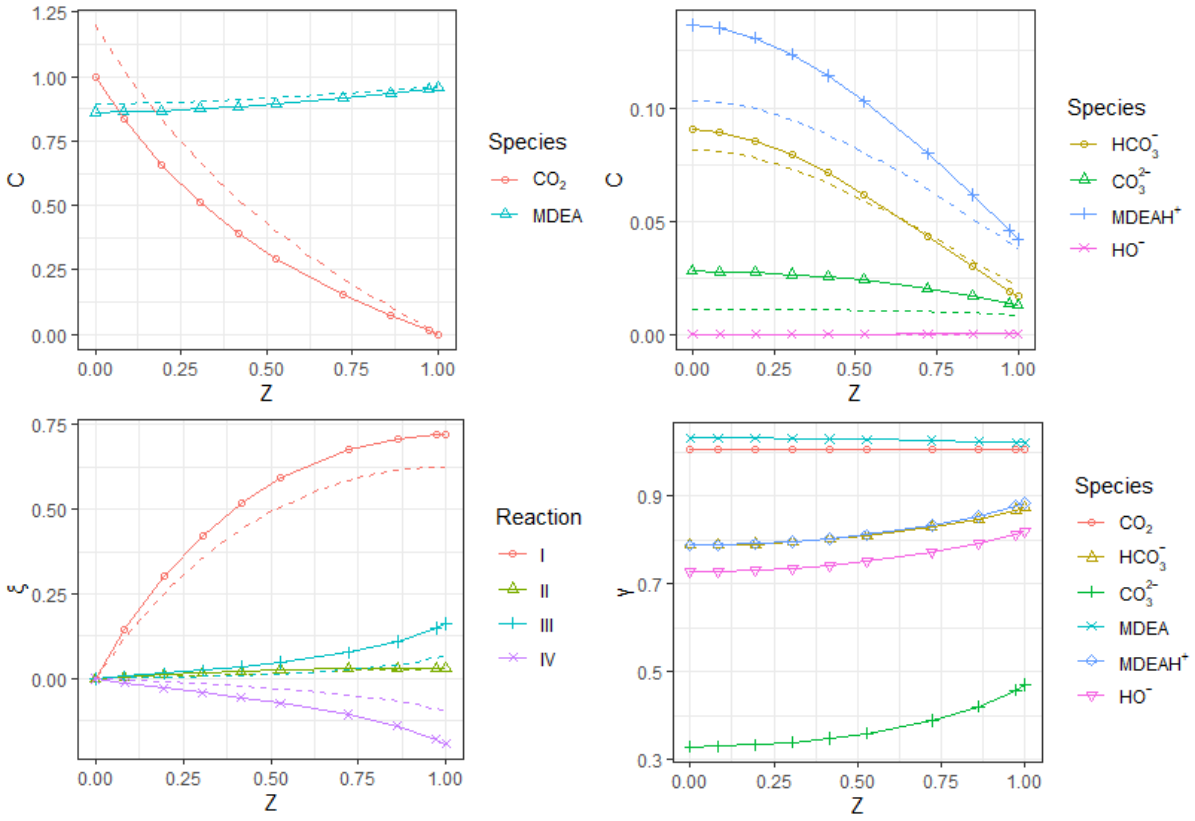

290

291 **Figure 7** Simulated CO_2 absorption in aqueous MDEA solution at $\omega_{MDEA,app}$ = 0.10 and α = 0.03
292 mol/mol MDEA, 300 K and P_{CO2} = 94.6 kPa measured by (Qian et Guo 2009). C: normalised
293 concentration, ξ: extent of reaction, γ: activity coefficient. Solid line & symbol: activity-based model,
294 dashed line: concentration-based model (C and ξ).

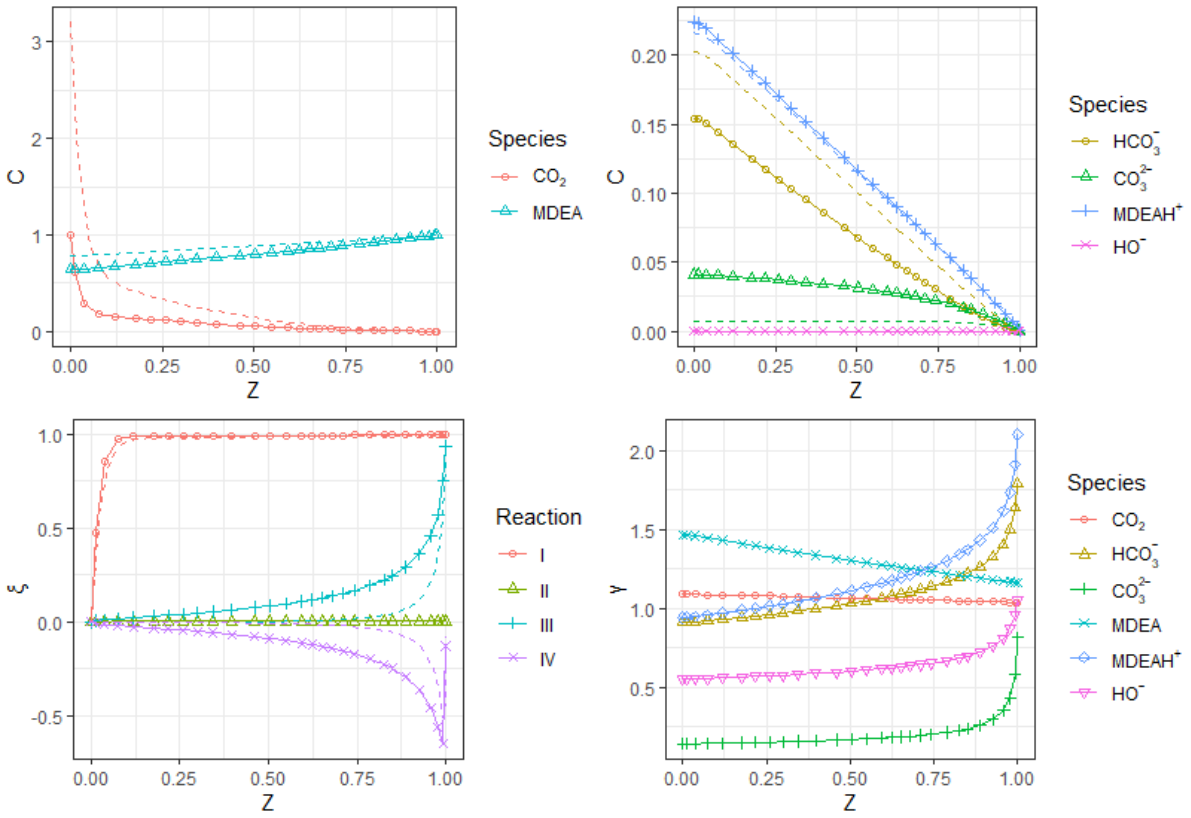

295

296 **Figure 8** Simulated CO_2 absorption in aqueous MDEA solution at $\omega_{MDEA,app}$ = 0.51 and α = 0 mol/mol
297 MDEA, 318 K and P_{CO2} = 104.9 kPa measured by (Pani, et al. 1997). C: normalised concentration, ξ:
298 extent of reaction, γ: activity coefficient. Solid line & symbol: activity-based model, dashed line:
299 concentration-based model (C and ξ).

300 For selected points at low CO_2 loading, concentration and extent of reaction profiles calculated with
301 non-ideality consideration (solid lines and symbols in Figure 7 and Figure 8) or with ideal solution
302 hypothesis (dashed lines in Figure 7 and Figure 8) display similar trends. In both cases, estimated CO_2
303 concentration at interface is higher in concentration-based model than in activity-based model.
304 However, the difference is way higher at $\omega_{MDEA,app}$ = 0.51 (Figure 8: +221%) than at $\omega_{MDEA,app}$ = 0.10
305 (Figure 7: +20%). This is linked to the thermodynamic representation of CO_2 physical solubility
306 discussed previously. Moreover, activity coefficients differ from unity in activity-based model and
307 significantly vary through the film, which is another difference factor with concentration-based
308 model.

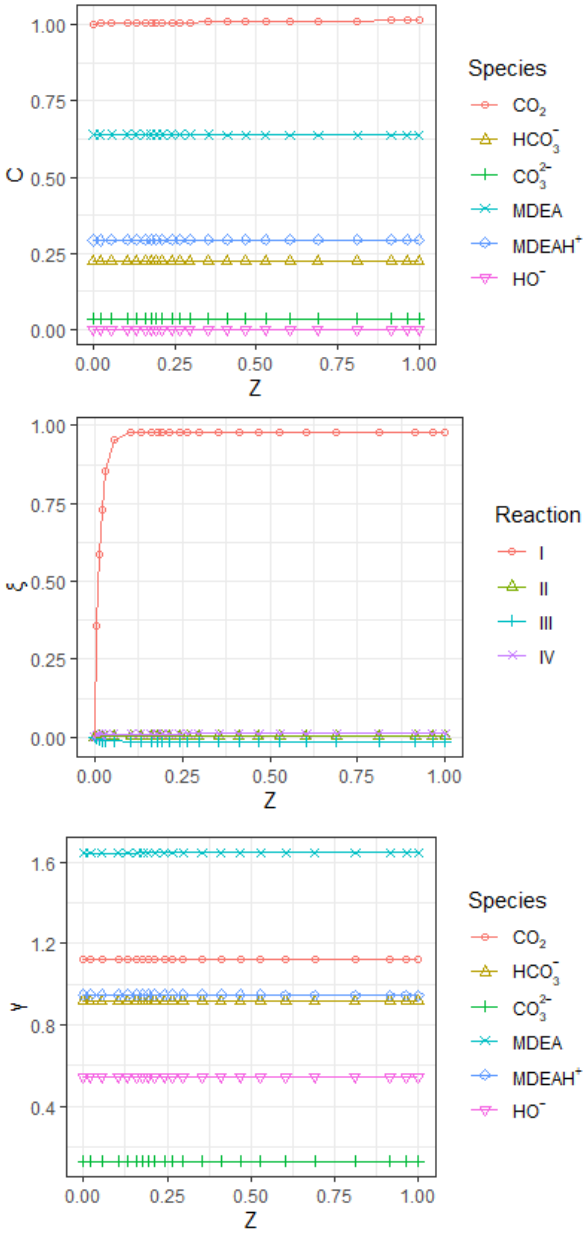

309

310 **Figure 9** Simulated CO_2 desorption from aqueous MDEA solution by the activity-based model at
311 $\omega_{MDEA,app}$ = 0.5 and α = 0.28 mol/mol MDEA, 332 K and P_{CO2} = 70.1 kPa measured by (Cadours 1998).
312 C: normalised concentration, ξ: extent of reaction, γ: activity coefficient.

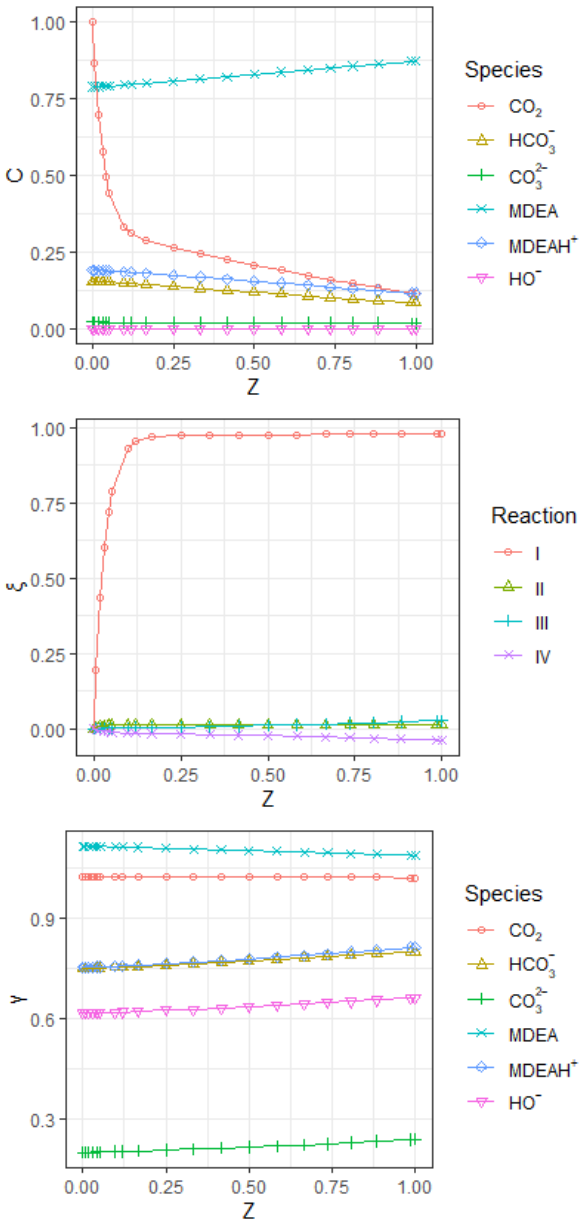

313

314 **Figure 10** Simulated CO_2 absorption in aqueous MDEA solution by the activity-based model at
315 $\omega_{MDEA,app}$ = 0.23 and α = 0.1 mol/mol MDEA, 333 K and P_{CO2} = 22.6 kPa measured by (Hamborg et
316 Versteeg 2012). C: normalised concentration, ξ: extent of reaction, γ: activity coefficient.

317 From all four extent of reaction plots, the reaction between CO_2 and HO^- ion (R-II) appears to have no
318 influence ($\xi_{II} \approx 0$). HO^- concentration is negligible, especially close to the interface.

319 Extents of acid-base reactions (R-III and R-IV) are significant in initially unloaded solutions. However,
320 contrary to alkaline salts systems studied in (Delgado, et al. 2023), CO_3^{2-} conversion through the film
321 remains marginal. HCO_3^- and $MDEAH^+$ are the main reaction products, even at low CO_2 loadings
322 where pH is highest.

323 The apparition of activity coefficient gradients seems much more influenced by
324 absorption/desorption driving force than by CO_2 loading, MDEA composition or temperature. In

Figure 7 and Figure 8, absorption into initially unloaded solutions at $\omega_{MDEA,app}$ = 0.10 and 0.51 and T = 300 and 332 K, with CO_2 driving forces of around 100 kPa (94.6 and 104.9 kPa) shows the highest activity coefficient gradients (especially $MDEAH^+$ and CO_3^{2-} activity coefficients). Additionally, at these conditions, an important drop in MDEA concentration at the interface takes place (respectively 0.10 and 0.51 of total MDEA mass fractions). Therefore, the "pseudo-first order absorption regime" assumption cannot apply.

On the other hand, profiles calculated in already loaded solutions (Figure 9 and Figure 10), with CO_2 driving forces below 20 kPa, either in the positive or negative, don't display any significant activity coefficient gradient. However, activity coefficients appreciably differ from unity. Although CO_3^{2-} is never a main product of CO_2 absorption or desorption, CO_3^{2-} activity coefficient is always lower than 0.5.

4. Conclusion

The current two-part study implements a steady-state reactive absorption model applied to the stagnant film theory and focusing on solution non-ideality representation in equilibrium relations, Nernst-Planck diffusion fluxes and reaction rates. This approach is more complete than literature models where activity coefficients are assumed constant, and most often equal to unity. Extents of reactions, a new feature for reactive absorption models, reduces the number of differential problem variables while maintaining a general formulation. This formulation with Nernst-Planck equation for molecular diffusion and activity-based rate expressions consists in a system of $n_C + n_{R,kin}$ first-order ordinary differential equations, whereas writing local balances per species leads to a system of n_C second-order differential equations. The relation between fluxes and extents of reactions is dictated by stochiometric constraints.

In (Delgado, et al. 2023), this model was first applied to alkaline salts-water-CO_2 systems and the CO_2 absorption flux data from the literature. In part II presented here, CO_2 absorption into aqueous MDEA solutions was studied. Firstly, a graphical data coherence analysis was carried out by plotting a flux density variable against CO_2 loading. Outliers from (Benamor et Aroua 2007) and (Pacheco et Kaganoi 2000) were then filtered out.

Then, using the selected data, Arrhenius parameters of the reaction between MDEA and CO_2 were optimised in both concentration- and activity-based models. Results emphasise the role of CO_2 physical solubility representation in reactive absorption model overall performance. N_2O-CO_2 analogy and activity-coefficient-corrected CO_2 Henry's constant in pure water lead to incompatible estimations of CO_2 interfacial concentration at high MDEA concentrations. This supports the need for global modelling: kinetic parameters should be used with all underlying parameters with which they were obtained. This is especially true when designing industrial columns.

For aqueous MDEA solutions, N_2O-CO_2 analogy is not proven theoretically. Having access to direct measurements of molecular CO_2 concentration in aqueous MDEA solutions would be beneficial to kinetic modelling. Such measurements exist for reactive systems, such as CO_2 in aqueous diethanolamine solutions (Diab, et al. 2012). In their absence, molecular simulation could provide estimates. Results of the present study suggest that amine concentration should be considered as well as water in CO_2 Henry's constant calculation at infinite dilution.

Lastly, simulated profiles through the liquid film indicate the relevance of the developed representation, especially considering the high deviation from ideality of the system and the apparition of activity coefficient gradients through the film at high absorption driving force. This implies kinetic parameters obtained at high absorption driving force with a simplified approach disregarding this effect could be incompatible with low absorption driving force experimental absorption/desorption flux data, and vice versa. This could be a factor impeding laboratory-scale data comparisons obtained at different absorption driving force conditions.

Acknowledgements

Pr. Alain Gaunand and Pr. Christophe Coquelet would like to acknowledge TotalEnergies for their research partnership and financial support, and the authors would like to acknowledge the Agence Nationale de la Recherche et de la Technologie (ANRT) for their financial support (CIFRE 2018/1069).

References

Benamor, A, et M K Aroua. «An experimental investigation on the rate of CO2 absorption into aqueous methyldiethanolamine solutions.» Édité par Springer. *Korean Journal of Chemical Engineering* 24, n° 1 (2007): 16-23.

Bottoms, R R. «Organic bases for gas purification.» *Industrial & Engineering Chemistry* 23, n° 5 (1931): 501-504.

Cadours, R. *Absorption-desorption de gaz acides par des solutions aqueuses d'amines.* Paris: ENSMP, 1998.

Camacho, F, S Sanchez, R Pacheco, M D La Rubia, et A Sanchez. «Kinetics of the reaction of pure CO2 with N-methyldiethanolamine in aqueous solutions.» Édité par Wiley Online Library. *International journal of chemical kinetics* 41, n° 3 (2009): 204-214.

Costa, C, M Demartini, R Di Felice, M Oliva, et P Pagliai. «Piperazine and methyldiethanolamine interrelationships in CO2 absorption by aqueous amine mixtures. Part I: Saturation rates of single-reagent solutions.» Édité par Wiley Online Library. *The Canadian Journal of Chemical Engineering* 97, n° 5 (2019): 1160-1171.

Delgado, S, A Gaunand, C Coquelet, R Cadours, et C Volpi. «A new reactive absorption model using extents of reaction and activities. I. Application to Alkaline-salts-CO2 systems.» *Chemical Engineering Science* 270 (2023): 118522.

Derks, P. W. J, T Kleingeld, C Van Aken, J A Hogendoorn, et G F Versteeg. «Kinetics of absorption of carbon dioxide in aqueous piperazine solutions.» *Chemical Engineering Science* 61, n° 20 (2006): 6837-6854.

399 Diab, F, et al. «Quantitative analysis of the liquid phase by FT-IR spectroscopy in the system
400 CO2/diethanolamine (DEA)/H2O.» *Fluid Phase Equilibria* 325 (2012): 90-99.

401 Donaldson, T, et Y Nguyen. «Carbon dioxide reaction kinetics and transport in aqueous amine
402 membranes.» *Industrial & Engineering Chemistry Fundamentals* 19, n° 3 (1980): 260-266.

403 Gondal, S, H F Svendsen, et H K Knuutila. «Activity based kinetics of CO2--OH- systems with Li+, Na+
404 and K+ counter ions.» Édité par Elsevier. *Chemical Engineering Science* 151 (2016): 1-6.

405 Hamborg, E S, et G F Versteeg. «Absorption and desorption mass transfer rates in chemically
406 enhanced reactive systems. Part I: Chemical enhancement factors.» Édité par Elsevier.
407 *Chemical engineering journal* 198 (2012): 555-560.

408 Jamal, A, A Meisen, et C J Lim. «Kinetics of carbon dioxide absorption and desorption in aqueous
409 alkanolamine solutions using a novel hemispherical contactor—I. Experimental apparatus
410 and mathematical modeling.» Édité par Elsevier. *Chemical engineering science* 61, n° 19
411 (2006): 6571-6589.

412 Kamps, A P-S, A Balaban, M Jödecke, N A S Kuranov, et G Maurer. «Solubility of single gases carbon
413 dioxide and hydrogen sulfide in aqueous solutions of N-methyldiethanolamine at
414 temperatures from 313 to 393 K and pressures up to 7.6 MPa: New experimental data and
415 model extension.» *Industrial & Engineering Chemistry Research* 40, n° 2 (2001): 696-706.

416 Kamps, A P-S, et G Maurer. «Dissociation constant of N-methyldiethanolamine in aqueous solution at
417 temperatures from 278 K to 368 K.» *Journal of Chemical & Engineering Data* 41, n° 6 (1996):
418 1505-1513.

419 Kierzkowska-Pawlak, H, et A Chacuk. «Kinetics of carbon dioxide absorption into aqueous MDEA
420 solutions.» *Ecol. Chem. Eng. S* 17, n° 4 (2010): 463-475.

421 Ko, J-J, et M-H Li. «Kinetics of absorption of carbon dioxide into solutions of N-
422 methyldiethanolamine+ water.» Édité par Elsevier. *Chemical engineering science* 55, n° 19
423 (2000): 4139-4147.

424 Lagarias, J C, J A Reeds, M H Wright, et P E Wright. «Convergence properties of the Nelder-Mead
425 simplex method in low dimensions.» *SIAM Journal on Optimization* 9, n° 1 (1998): 112-147.

426 Littel, R J, W P M Van Swaaij, et Geert F Versteeg. «Kinetics of carbon dioxide with tertiary amines in
427 aqueous solution.» Édité par Wiley Online Library. *AIChE Journal* 36, n° 11 (1990): 1633-1640.

428 Pacheco, M A, et S Kaganoi. «CO2 absorption into aqueous mixtures of diglycolamine and
429 methyldiethanolamine.» Édité par Elsevier. *Chemical engineering science* 55, n° 21 (2000):
430 5125-5140.

431 Pani, F, A Gaunand, R Cadours, C Bouallou, et D Richon. «Kinetics of absorption of CO2 in
432 concentrated aqueous methyldiethanolamine solutions in the range 296 K to 343 K.» Édité
433 par ACS Publications. *Journal of Chemical & Engineering Data* 42, n° 2 (1997): 353-359.

Pohorecki, R, et W Moniuk. «Kinetics of reaction between carbon dioxide and hydroxyl ions in aqueous electrolyte solutions.» *Chemical Engineering Science* 43, n° 7 (1988): 1677-1684.

Qian, Z, et K Guo. «Modeling and kinetic study on absorption of CO2 by aqueous solutions of N-methyldiethanolamine in a modified wetted wall column.» (Elsevier) 17, n° 4 (2009): 571-579.

Rangwala, H A, B R Morrell, A E Mather, et F D Otto. «Absorption of CO2 into aqueous tertiary amine/MEA solutions.» Édité par Wiley Online Library. *The Canadian journal of chemical engineering* 70, n° 3 (1992): 482-490.

Rinker, E B, S A Sami, et O C Sandall. «Kinetics and modelling of carbon dioxide absorption into aqueous solutions of N-methyldiethanolamine.» Édité par Elsevier. *Chemical Engineering Science* 50, n° 5 (1995): 755-768.

Rozanska, X, E Wimmer, et F de Meyer. «Quantitative kinetic model of CO2 absorption in aqueous tertiary amine solvents.» *Journal of Chemical Information and Modeling* 61, n° 4 (2021): 1814-1824.

Sheng, M, et al. «Effective Mass Transfer Area Measurement Using a CO2–NaOH System: Impact of Different Sources of Kinetics Models and Physical Properties.» *Industrial & Engineering Chemistry Research* 58, n° 25 (2019): 11082-11092.

Tomcej, R A, et F D Otto. «Absorption of CO2 and N2O into aqueous solutions of methyldiethanolamine.» Édité par Wiley Online Library. *AIChE journal* 35, n° 5 (1989): 861-864.

Versteeg, G F, et W PM van Swaaij. «On the kinetics between CO2 and alkanolamines both in aqueous and non-aqueous solutions—II. Tertiary amines.» Édité par Elsevier. *Chemical Engineering Science* 43, n° 3 (1988): 587-591.

Versteeg, G F, et W PM Van Swaaij. «Solubility and diffusivity of acid gases (carbon dioxide, nitrous oxide) in aqueous alkanolamine solutions.» Édité par ACS Publications. *Journal of Chemical & Engineering Data* 33, n° 1 (1988): 29-34.

Vinel, D J, et C Bouallou. «Propriétés physico-chimiques des solutions aqueuses d'alcanolamines utilisées dans le traitement du gaz.» *Scientific Study & Research* 1 (2004): 2.

Whitman, W G. «The two-film theory of gas absorption.» *Chemical & Mellaurgy Engineering* 29 (1923): 146-148.

Zhang, Y, et C-C Chen. «Thermodynamic Modeling for CO2 Absorption in Aqueous MDEA Solution with Electrolyte NRTL Model.» *Industrial & Engineering Chemistry Research* (American Chemical Society) 50, n° 1 (2011): 0888-5885.